Characterization of Celluloic-Based Polymer of Pentaclethra macrophylla Benth Pod (PMBP) and its Copper(II) ion Adsorption Performance

Dr. Okechukwu Paul Nsude
Enugu State University of Science and Technology
Dr. Kingsley John Orie (orie_john@uniport.edu.ng)
Ignatius Ajuru University of Education
Dr. Elechi Owhoeke
University of Port Harcourt

Research Article

Keywords: Adsorption, Celluloic-Based Polymer, Copper(II) ion, Pentaclethra macrophylla Benth, Pod

Posted Date: March 8th, 2023

DOI: https://doi.org/10.21203/rs.3.rs-2650345/v1

Additional Declarations: No competing interests reported.

Characterization of Celluloic-Based Polymer of *Pentaclethra macrophylla Benth* Pod (PMBP) and its Copper(II) ion Adsorption Performance

Okechukwu Paul Nsude[1], Kingsley John Orie[2*] and Elechi Owhoeke[3]

[1]Department of Industrial Chemistry, Enugu State University of Science and Technology,Enugu State, Nigeria.
[2]Department of Chemistry, Ignatius Ajuru University of Education, Rivers State, Nigeria

[3]Department of Industrial Chemistry/Petrochemical Technology, University of Port Harcourt Nigeria

Email address:
oriekingsley81@gmail.com
[*]Corresponding author

Abstract
The interest in cellulosic-based polymer materials is rapidly growing, both in industrial and basic research applications. This is based on its availability, renewability, low density, cheapness, biodegradability, and satisfactory mechanical properties. The research reports on the characterization of cellulosic-based polymers and copper (II) ion removal via *Pentaclethra macrophylla Benth* Pod (PMBP). Cellulose was successfully isolated from PMBP biomass *via* delignification and bleaching. X-ray diffraction (XRD), scanning electron microscopy (SEM), Fourier Transform Infrared Spectrometry (FTIR), thermal gravimetric analysis (TGA), and deformation gravimetric analysis (DGA) were used to characterise the raw and isolated cellulose. The adsorbents were further characterized using adsorption isotherms, kinetics, and thermodynamic models. The isolated cellulose has better thermal stability, crystallinity, and porosity than the raw cellulose. The removal of the matrix material (most hemicelluloses and almost all the lignin) led to an increase in the crystallinity, morphology, and maintenance of the thermal stability of the cellulosic-based polymer. The functional group elucidation showed that both raw and isolated contained cellulose, hemicelluloses, and lignin. The kinetic investigation was fitted with a pseudo second-order model. Thermodynamic parameters affirmed that the evacuation of Cu(II)ions was plausible, unconstrained, and exothermic in nature. The adsorption isotherm, kinetics, and thermodynamic studies show that both raw and cellulosic-based polymers can serve as Cu(II) ion removers, with a preference for cellulosic-based polymers. It therefore implies that cellulosic-based polymers obtained from PMBP could be used for copper (II) ion removal in water and industrial waste.

Keywords: Adsorption, Celluloic-Based Polymer, Copper(II) ion, *Pentaclethra macrophylla Benth,* Pod

Introduction
The current global drive to promote renewable agri-resources research and innovation has resulted in the development of novel and high-value products based on cellulosic-based polymers. Cellulose is the most prevalent of all naturally occurring organic compounds, with an extreme high annual production [1]. It is a linear polymer of glucose unit monomers. It is a polysaccharide (polymer) composed of monomers (simple sugars) linked together to form very massive molecules [2, 3]. The cellulose repeat unit is connected together by oxygen covalently bound to C_1 of one glucose ring and C_4 of the next ring. Plant fibres like cotton,

hemp, flax, and jute, as well as wood, which contain 42% cellulose, are the main sources of cellulose. It is insoluble in water and easily separated from the other plant elements [3, 4].

Pentaclethra macrophylla Benth is a tree native to Nigeria's southern and middle belt areas, as well as other West and Central African coastal locations. It is a member of the Leguminosae family and the Mimosoideae subfamily [5, 6]. According to the literature, *Pentaclethra macrophylla benth* unfermented seed oil contained fatty acids [6,] important mineral elements (phosphorus and calcium) [7], vitamins (thiamin, riboflavin, and niacin) [8,] carbohydrates, and amino acids (stachylose, galactose, and fructose). In the eastern part of Nigeria, biomass waste from Pentaclethra macrophylla Benth pod/husk is dumped indiscriminately, contributing to environmental contamination. Madukasi et al. [8] evaluated PMBP as an energy source with a calorific value of 3456 kcal/kg. The elemental analysis reveals that PMBP is safe for the environment and can be used as a feed substrate for livestock [9].

A few studies have recently been conducted in an attempt to obtain pure cellulose from specific parts of the date palm. Alothman et al. [9] isolated microcrystalline cellulose from date palm seeds, estimating the cellulose crystallinity index to be 62% before acid hydrolysis and 72% after acid hydrolysis. Microcrystalline cellulose was recovered from sugarcane bagasse employing a bleaching agent, alkali, and acid hydrolysis in a related investigation. The crystallinity index of sugarcane bagasse cellulose was estimated to be 79.49% [10, 11]. Another study recovered cellulose from discarded bambo fronts, leaflets, and fibres using dilute acid, alkali, and bleaching with acetic acid, hydrogen peroxide, and sulphuric acid, with a raw crystallinity index of 52.27% and a modified index of 70% for alpha-cellulose [12, 13].

Some studies have used different traditional approaches to eliminate hazardous pollutants. Physical methods typically employed in this regard include ion exchange, filtration, membrane separation, evaporation, and reverse osmosis [13, 14]. Both physical and chemical approaches demand a large initial investment and a high operating cost, and they are challenging to utilise in environments with low heavy metal concentrations [15, 16]. Adsorption is the most commonly used heavy metal removal method among various chemical and physical methods because of its unique characteristics, such as simplicity, environmental friendliness, economic feasibility, no sludge formation, high efficiency, regeneration, a wide range of adsorbent availability, and low initial investment [16].

Adsorbent is essential in the removal of heavy metals during the adsorption process. Adsorbents can remove pollutants by interacting with them physically or chemically. Adsorption has been shown to be effective in removing trace amounts of Cu(II) ions from effluent or wastewater [17]. Most agricultural wastes, biological wastes such as bacteria, algae, and fungi, fruit peels, and so on, have recently been used as adsorbents for the removal of various colours and metals from natural resources. Biosorbents are natural materials that are primarily waste and produce better outcomes than typical adsorbents, ion exchange resins, and activated carbons. Biosorbents are significantly less expensive and more environmentally friendly than other adsorbents [18–21]. Delonix regia seeds (DRS) can be employed as a biosorbent due to their increased porosity and diverse functional groups, which include carbohydrates, particularly polysaccharides, and proteins, which aid in the removal of Cu(II) ions from tannery effluent [22, 23].

The purpose of this study is to characterize cellulosic-based polymers from PMBP biomass wastes for use in the adsorption of copper (II) ions. The adsorbents (raw and cellulosic-based polymers) were characterized with FTIR, SEM, XRD, and TG/DTG and were used as adsorbents for the removal of Cu(II) ions from the synthetic solution. A batch experimental study was carried out, and the interactive behaviour between the adsorbent and Cu(II) ions was explained via an isotherm study using different adsorption isotherm models (Langmuir, Freundlich, and Temkin). The adsorption rate mechanism for the removal of Cu(II) ions onto adsorbents was examined using different kinetic models such as pseudo-first-order, pseudo-second-order, and particle diffusion models, and finally, the thermodynamic nature of the adsorption study was determined by the thermodynamic study.

2.0 Material and Methods

2.1 Materials

The natural *pentaclethra macrophylla benth* pod (PMBP), Potassium hydroxide (KOH), hydrochloric acid (HCl), ethanol, toluene, acetic acid, sodium chlorite, NaOH and other chemicals were analytical grade. All the chemicals were used as received. Deionized water was used in all experiments

2.2 Sample collection and Preparation

The *pentaclethra macrophylla benth* pod (PMBP) was gathered in Aku, Igbo Etiti Local Government Area, Enugu State, and transported to the department of Industrial chemistry laboratory, University of Science and Technology, Enugu. It was carefully sorted to eliminate foreign material from the sample. To prepare for pulverisation, the sample was rinsed with distilled water, sun-dried for 2-3 weeks, and then chopped with a cutter. To increase the surface area and improve future treatment, the sun-dried chopped pod sample of PMB was crushed into fine powder and sieved to particle sizes of 0.07 mm.

2.2 Dewaxing of *Pentaclethra Macrophylla Benth* Pod (PMBP)

The dewaxing technique used was consistent with Nsude et al. [4]. The powdered PMBP sample (100g) was extracted for 6 hours with 375 ml of toluene and ethanol (2:1) using a soxhlet extractor to remove chlorophyll pigments and waxes. After removing the boiling chips, the filtrate (toluene-ethanol combination) was discarded. The residue (dewaxed PMS) was dried at room temperature, weighed, and stored in a sealed plastic bag for further analysis.

2.4 Bleaching of the cellulose residue PMBP

The resulting sample residue was bleached for 30 minutes at 70 ^{o}C using an aqueous solution of sodium hypochlorite (7.5%). The resulting holocellulose was extensively cleaned and filtered. The resultant holocellulose was then treated with 17.5% w/v sodium hydroxide at 80 ^{o}C for 30 minutes. The cellulose pulp was thoroughly rinsed with water. The cellulose pulp was whitened further by employing a 1:1 aqueous solution of sodium hypochlorite (3.5 % w/v) for 5 minutes at 100 ^{0}C, followed by washing until the filtrate was clear. Excess water was manually squeezed out using a calico cloth, and the alpha-cellulose pulp was oven-dried at 50 ^{0}C [23].

2.5 Characterizations

2.5.1 Scanning Electron Microscope

The morphological feature of the cellulose was observed using scanning electron microscope (SEM, FEI, Quanta 200, USA), transmission electron microscope (TEM, FEI, Tecnai G20, USA).

2.5.2 Fourier Transform Infrared

The IR spectra were obtained from the FTIR-8400S Fourier Transform Infrared spectrophotometer at NARICT Zaria using an ATR disc. It was used to identify the functional groups,

2.5.3 X-ray Diffraction

The crystalline structures of cellulose samples were determined by XRD technique. XRD analysis was carried out using a Bruker D8 ADVANCE Powder XRD instrument with CuK-α radiation of λ = 1.5404 nm and the X-ray diffractometer was operated at a voltage of 40 kV and a current of 30 mA. XRD data were collected within the range of scattering angles (2θ) of 10 to 40° at room temperature.

Crystallinity index (CrI) was calculated using the formula as stated in Equation 1:

$$CrI\ (\%) = [(I_{200} - I_{CAM}) / I_{200}] \times 100 \quad (1)$$

Where I_{200} and $I_{Cr\text{-}non}$ are the maximum peak intensities of crystalline and amorphous regions, respectively [20].

2.5.4 Thermogravimetric Analysis

TG/DTG curves were obtained using Seiko EXSTAR 6000 TG/DTA 6300 thermal analyzer. Approximately 10.2 mg of samples were placed on an aluminum pan for testing. This test was carried out from 30 to 900 °C in dynamic nitrogen atmosphere with the flow rate of 10 ml/min and heating rate of 10 °C/min

2.5.5 Atomic absorption spectrophotometer (AAS) MODEL: FS240A analysis

100 ml of well shaken water sample was transferred into a glass beaker of 250 ml volume, 5 ml concentration of nitric acid was next added and boil until volume reduced to 15-20 ml, addition of concentrated nitric acid drop wise continued until the residue were completely dissolved. The mixture is cooled, transferred and made up to 100ml using metal free distilled water; a calibration graph is obtained by feeding the standard solutions of suitable concentration. The samples are aspirated by feeding them through the capillary and the readings were noted.

3.6 Adsorption Capacity

The adsorption capacity that is the metal ions adsorbed onto the resin was calculated using mass balance relation as in equation 2

$$Q_e = \frac{(C_o - C_e)V}{M} \quad (2)$$

Where: Q_e(mg/g) is the adsorption capacity of the adsorbent; C_o and C_e (mg/l) are the initial and final concentration of the metal ions in solution phase, V is the volume of the aqueous solution (l)

M is the weight of the adsorbent (g),

The percentage of ions removed was calculated as thus 3

$$\%\ of\ ions\ Adsorbed = \frac{(C_o - C_e)}{C_o} \times 100 \quad (3)$$

3.7 Adsorption Isotherms

Results obtained from the ion adsorption experiments Cu^{2+}, $Pb^{2+}$and Fe^{2+} of ions were studied using adsorption models of Langmuir, Freundlich and Temkin adsorption isotherms.

3.7.1 Langmuir's isotherm

The formula for Langmuir's model equation is

$$\frac{C_e}{Q_e} = \frac{C_e}{Q_m} + \frac{1}{bQ_m} \quad (4)$$

The model equation can also be rewritten as

$$\frac{C_e}{Q_e} = C_e\left[\frac{1}{Q_m}\right] + \frac{1}{bQ_m} \quad (5)$$

Where:C_e is the metal ion concentration at equilibrium (mg/l); Q_e is the adsorption capacity at equilibrium (mg/g); Q_m is the maximum adsorption capacity (mg/g); b is the Langnuir equilibrium constant related to the affinity of the building sites (l/mg).

$\frac{C_e}{Q_e}$is plotted against C_e to get slope$\frac{1}{Q_m}$ and intercept $\frac{1}{bQ_m}$ from which b and Q_m are calculate indicating that adsorption follows the Langmuir isotherm and conformation of the experimental data into Langmuir isotherm indicates the homogenous nature of the adsorbent surface. The essential characteristics of the Langmuir isotherm can be expressed in terms of a dimensionless equilibrium parameter (R_L) [24] which is defined by;

$$R_L = \frac{1}{1+bC_o} \quad (6)$$

Where, b is the Langmuir constant and C_0 is the adsorbate concentration (mg/l). The value of (R_L = 1) or favourable (0 < R_L<1) or irreversible (R_L = 0).

3.7.2 Freundlich Isotherm

Adsorbent that follow the Freundlich isotherm equation are assumed to have heterogeneous surface consisting of sites with different adsorption potentials, each type of site is assumed to adsorbed molecules, as in adsorption isotherm represents the relationship between the amount of metal adsorbed per unit mass of the adsorbent and the concentration of the metal in solution at equilibrium[25]

The Freundlich adsorption's equation is given by:

$$\log Q_e = \log K_F + \frac{1}{n}\log C_e \quad (7)$$

Where K_F and n are Freundlich constants, n giving an indication of how favourable the adsorption process is and K_F is the adsorption capacity of the adsorbent while $\frac{1}{n}$ shows the intensity of adsorption. K_F and n are determined from the linear plot of $\log Q_e$ versus $\log C_e$

3.7.3 Temkin Isotherm

This model ignores extremely low and large concentration values. The model assumes that heat of adsorption (function of temperature) of all the molecules in the layer would decrease linearly rather than logarithmic with coverage; its derivation is characterized by a uniform distribution of binding energies [25]

The equation for Temkin isotherm model is given by

$$q_e = \frac{RT}{bT}\ln(A_T C_e) \quad (8)$$

Rearranging equation 3.20

$q_e = \frac{RT}{bT}\ln(A_T) + \frac{RT}{bT}\ln(C_e)$ (9)

$\beta = \frac{RT}{bT}$ (10)

$q_e = \beta \ln A_T + \beta \ln C_e$ (11)

Where A_T is Temkin isotherm equilibrium binding constant (l/g); b_T is Temkin isotherm constant; R is the universal gas constant (8.314Jmol^{-1}K^{-1})

T is temperature; B is constant related to heat of sorption (J/mol)

3.8.1 Pseudo First – Order Kinetic Model

The pseudo first-order equation is stated below[26]

$ln\ (Q_e - Q_t) = ln\ Q_e - (K_1)t$ (12)

Where

K_1 (min^{-1}) is the rate constant of the pseudo first-order sorption, Q_1 (mgg^{-1}) denote the amount of sorption at time t (min), Q_e (mgg^{-1}) is the amount of sorption at equilibrium

3.8.2 Pseudo Second – Order Kinetic Model

The Pseudo second-order equation can be written as given below by Rao et al. [26]:

$\frac{t}{q_t} = \frac{1}{v_o} + \left(\frac{1}{q_e}\right)t$ (13)

Where;

v_o = $K_2 q_e^2$ (mg g^{-1}min^{-1}) is the initial sorption rate, K_2 (g mg^{-1} min^{-1}) correspond to the rate constant of sorption, q_e (mg g^{-1}) is the amount of metal ion adsorbed at equilibrium, q_t (mg g^{-1}) is the amount of metal ion on the surface of the sorbent at any time t (min).

3.9 Thermodynamics of Adsorption

Thermodynamic parameters ΔH, ΔS and $\Delta G$are calculated using equation 14

$\ln \frac{Q}{C_e} = \frac{-\Delta H}{RT} + \frac{\Delta S}{R}$ (14)

R is the Gas law constant = 8.314J (mol K^{-1}) and T is the temperature in Kelvin (K)

$\Delta H$and ΔS are determined from the slope and intercept respectively of the linear plot of $\frac{Q}{C_e}$ versus $\frac{1}{T}$. Gibbs free energy of adsorption ΔG (KJ/mol) is calculated from the values of ΔH and ΔSusing equation 15[26,27]

$\Delta G = \Delta H - T\Delta S$ (15)

3.0 Result and discussion

3.1 X-ray Diffraction and Crystal Structure Analysis of Cellulose from PMBP

The crystallinity of cellulose determines its mechanical and thermal properties as a reinforced component in polymer composites. In Figures 1a and 1b, XRD analysis estimated the crystallinity of the raw PMBP powder and isolated cellulose composites of PMBP. For raw powder, the intense peak around 2θ = 20° (I200), represents the crystalline region of the samples, whereas the peak around 2θ = 15.4° (Iam) represents the amorphous region of the powder samples. After alkaline treatment and bleaching of the raw PMBP powder, the isolated cellulose has a crystalline region of around 2θ = 34° (I200), whereas the amorphous

region is around 2θ = 23° (Iam). This finding was consistent with Akinjkun et al. [27], who identified the crystalline region of untreated cellulose in cocoa pod husk or eggshell to be 2θ = 30° (I200) and the amorphous region as 2θ = 26° (Iam).
As a result, the isolated cellulose displayed additional peaks at 40 0C and 58 OC, comparable to what Rosli et al., [28] reported as crystallographic planes of cellulose 1 polymorph, showing that the isolated cellulose possesses typical cellulose I structure. The crystallinity index (CrI) of raw PMBP powder and isolated PMBP cellulose was determined to be 23% and 32.4%, respectively. This clearly demonstrates that progressive chemical treatments increase the crystallinity of isolated cellulose.

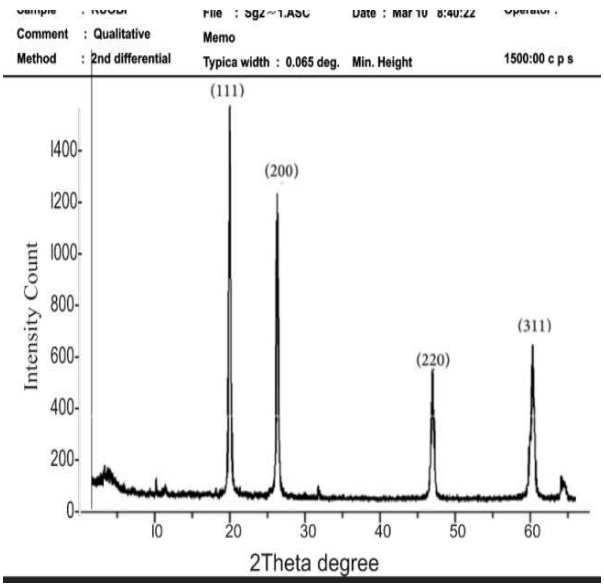

(1a)

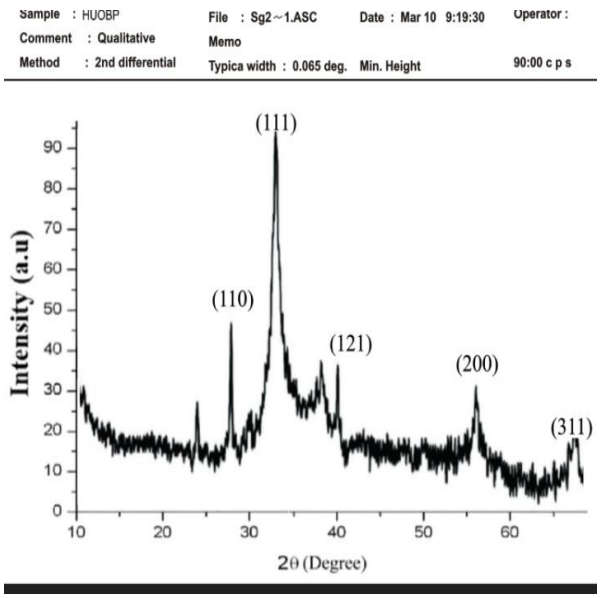

(1b)

Figure 1: (a) XRD Diffractograms of PMBP and (b) XRD Diffractograms of PMBP-C

3.2 Morphological Analysis of Raw and Cellulose from PMBP Biomass

SEM was used to examine the morphology of the PMBP biomass at various stages of the chemical treatment. Figures 2a and 2b show SEM micrographs of raw PMBP powder and isolated cellulose at various stages of processing and magnifications (900x and 1000x). The micrograph became clearer as the picture size increased, and it was also observed that the image appeared intertwined and bound together [29]. It is possible that the raw materials' lignocellulosic structure is not apparent because they are still coated or cemented with wax, hemicelluloses, pectin, and lignin, among other impurities and components. The morphology analysis of cocoa pod husks by Akinjokun et al. [27] that attributed the layered or cemented structure to impurities due to wax, hemicellulose, pectin, and lignin is consistent with this finding.

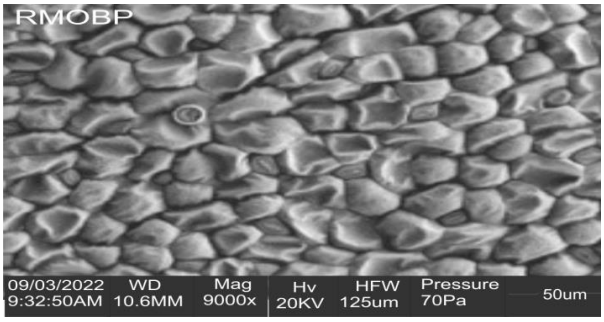

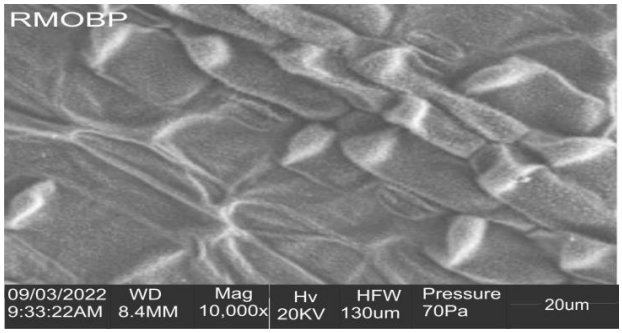

(2a)SEM Micrograph Analysis for Raw PMBP

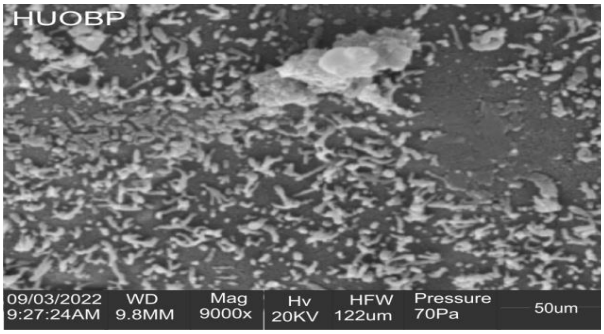

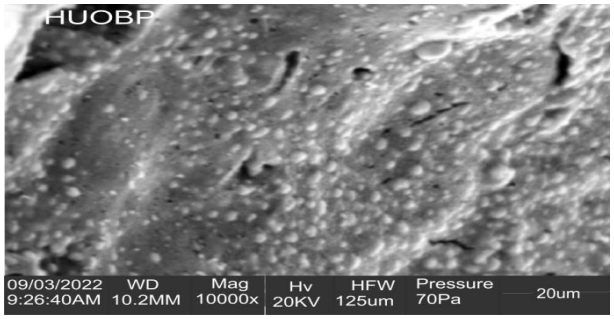

(2b)Micrograph Analysis of modified PMBP-C

Figure 2: SEM Micrograph Analysis for Raw and Isolated Cellulose PMBP

3.3 Thermagravimetric Analysis (TGA) and Deformation Gravimetric analysis (DGA)

Figure 3 shows the thermogravimetric (TGA) and deformation gravimetric (DTA) results of raw PMBP powder and separated cellulose of PMBP biomass as a function of temperature and weight loss. Figures 3a and 3b show TGA of raw powder and isolated cellulose, while Figures 3c and 3d show DGA of raw powder and isolated cellulose. The two samples demonstrate three distinct areas of weight reduction. Figure 3a shows a modest decrease in percentage weight loss, which is clearly visible in Figure 3c (DTG). The evaporation of adsorbed moisture on the surfaces of the materials, as well as chemisorbed and hydrogen bound water molecules in the samples, has been linked to the decrease in % weight observed in this temperature range of 20–130 ^{o}C [30, 31]. It may also be related to the volatilization of low molecular weight chemical molecules in raw PMBP powder and residual hemicellulose in separated cellulose [30]. The thermal degradation of the raw PMBP powder began at about 280 ^{o}C and reached a maximum around 435 ^{o}C, accounting for cellulose pyrolysis in the sample, according to the TG curve in Figure 3a. Thermal breakdown began at 260 ^{o}C in the case of isolated cellulose from PMBP produced after alkali treatment and bleaching (Figure 3d). This is less than the values reported in the literature for cellulose isolated from mulberry tree bark [32] and cocoa pod husk [33], but comparable to the value reported by Sheltami et al. [30] for cellulose recovered from mengkuang leaves. The lower degradation initiation temperature for isolated cellulose from PMBP found in this investigation could be due to the residual hemicellulose component left over following the chemical treatment. In the DTG (Figure 3e), the separated cellulose exhibits a maximum peak temperature of roughly 375 ^{o}C. Lignolysis is associated with decomposition at temperatures above 400 ^{o}C. According to the

decomposition at 435 °C, the raw PMBP powder has more lignin, whereas the isolated cellulose has more cellulose and fewer hemicelluloses. The chemical treatment is responsible for the lignin reduction.

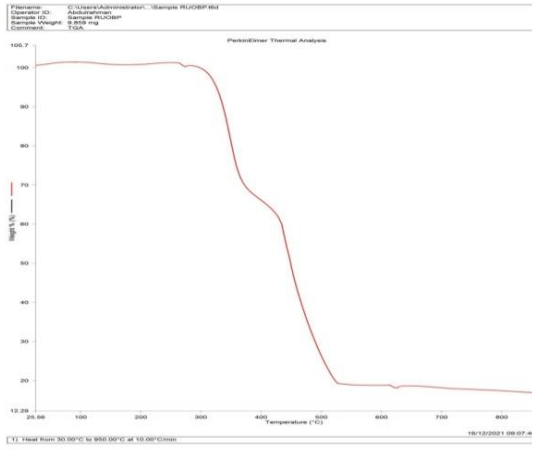

(3a)Thermagravimetric analysis (TGA) Raw PMBP

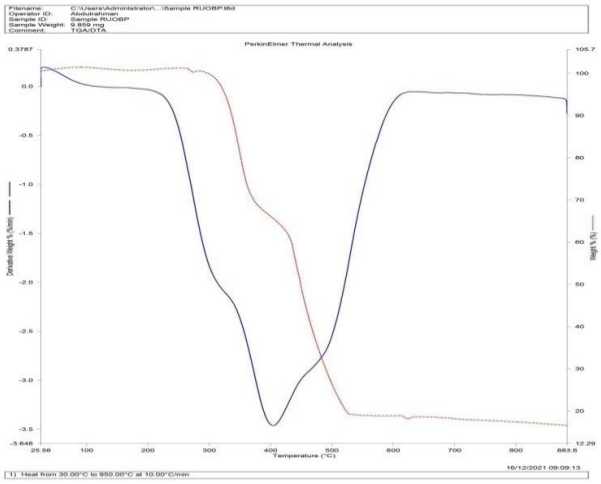

(3b)Deformation gravimetric (DGA) of Raw PMBP

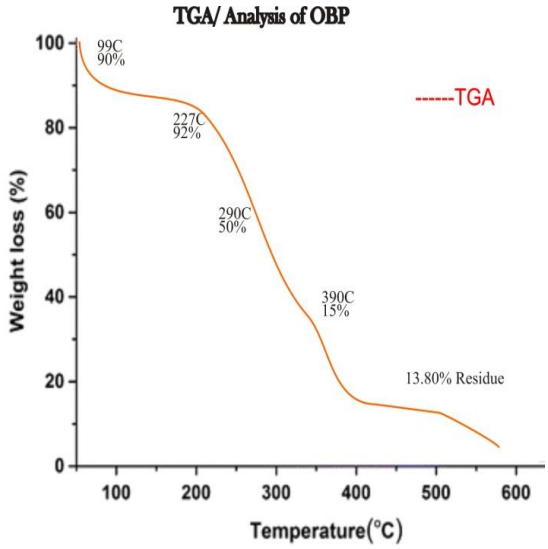

(3c)Thermagravimetric analysis (TGA) of isolated cellulose PMBP

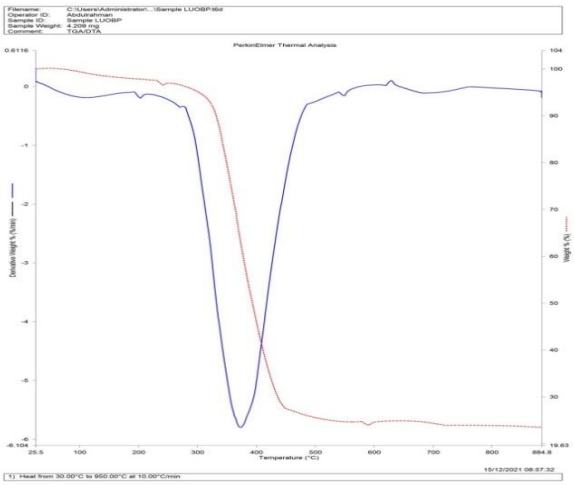

(3d)Deformation gravimetric (DGA) of isolated cellulose PMBP.

Figure 3: Thermagravimetric and Deformation gravimetric analysis Raw and Isolated PMBP

3.4 ATR-FTIR Analysis of Raw and Isolated Cellulose from PMBP Biomass

Table 1 shows the functional group analysis of both raw PMBP powder and the isolated cellulose of PMBP biomass.

Table 1: Summary of Functional Group Analysis of PMBM Biomass

	Functional Groups	Absorption(s) frequency(cm^{-1})
1	OH hydroxyl group	3446 - 3250
2	C-H stretch	2960-2850
3	C=O stretching of carboxylic acid or ester (lignin)	1750-1735
4	C=C stretching of aromatic ring (lignin)	1470-1350
5	CH_2 symmetrical bending (lignin)	1430-1330
6	C-O stretching of acetyl (lignin)	1245-960
7	β-glycosidic linkage	1000-980
8	-Si-O-C- stretching	1250-1100
9	-Si-C- symmetric stretching	800-750
10	-Si-O-Si-	720-700

The wide band with a maximum at 3550–3200 cm^{-1} is assigned to the O–H group. The peak at 1000-980 cm1 in all spectra represents the β-glycosidic connections of the glucose ring in cellulose [32, 34]. The band at 720-700 cm^{-1} detected in all sample spectra is assigned to the -Si-O-Si-, indicating the presence of silicon compound on both raw PMBP powder and isolated cellulose. While the bands at 2960-2850 cm^{-1} are caused by carbohydrate C-H rocking vibrations, which indicate the presence of organic molecules in the samples, and water O-H bending vibrations [34, 35], Other peaks identified are shown in Table 1. The overall FTIR spectra confirmed the presence of cellulose in PMBP biomass, with some trace of hemicelluloses and lignin..

3.5 Adsorption studies

3.5.1 Langmuir Adsorption Isotherms of Cu^{2+} Celluloic-Based Polymer of PMBP

The Langmuir adsorption isotherm of celluloic-based polymer of Cu (II) ion is shown in Table 2.

Table 2 Langmuir Isotherm parameters for the adsorption of Cu(II) ion on PMBP

	Adsorbents	**K or b (J/mol)**	**q_{max} (mg/g)**	**R_L**	**R^2**
1	PMBP-R	0.0532	40.650	0.2732	0.9888
2	PMBP-C	0.1099	42.194	0.154	0.8346

K or b= Langnuir equilibrium constant, q_{max} = maximum adsorption capacity, R_L= dimensionless equilibrium parameter, R=Correlation parameter

The Langmuir constants qmax and b were calculated using the Ce/Qe versus Ce plots shown in Figures 4a and 4b with linear regression coefficient values. From Table 2, it was observed that the interaction between the PMBP adsorbents and the adsorbate (Cu^{2+}) was generally poor, as seen in the values of K and q_{max}. However, the isolated celluloic-based polymer has better interaction with the adsorbates than the raw PMBP adsorbent. This is consistent with Ushakumary and Madhu [36], and Volesky [37].

Based on the Langmuir model, the treated adsorbents have a higher adsorption capacity than the raw PMBP. This could be associated with an increase in the surface area of the isolated celluloic-based polymer. This is in line with Azouaou et al. [38], who worked on different

adsorbents of biomass origin. The value of RL indicates whether the isotherm is unfavourable (R_L > 1), linear (R_L ¼ 1), favourable (0 < RL < 1) or irreversible (RL ¼ 0) [39]. From the R_L values (Table 1) and the range of metal ion concentrations (50-250 mg/l) tested, it follows that R_L lies between 0 and 1, which implies that the adsorption was favourable.

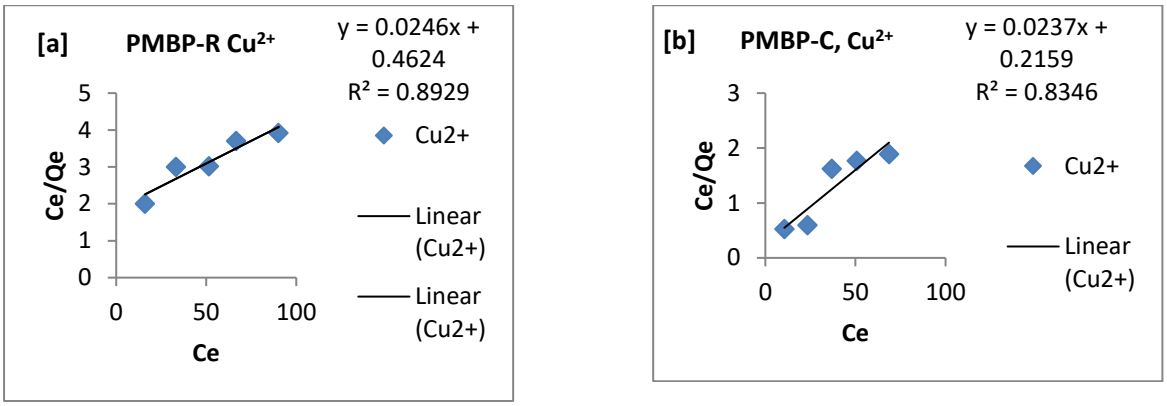

Figure 4: Langmuir adsorption of Cu^{2+} using PMBP

3.5.2 Freundlich Adsorption Isotherms of Cu^{2+} Celluloic-Based Polymer of PMBP

In a Freundlich adsorption isotherm, the adsorbate forms a monomolecular layer on the surface of the adsorbent. Table 3 shows the different adsorbents of PMBP and the Freundlich isotherm constants of Cu(II) ion.

Table 3: Freundlich Isotherm parameters for the adsorption of Cu(II) Ion on PMBP

	Adsorbents	K_f	1/n	R^2
1	PMBP-R	1.8314	0.9125	0.9969
2	PMBP-C	1.3140	0.8435	0.9975

The Freundlich adsorption isotherm constants K_f and 1/n were determined from the $\log Q_e$ versus logCe plot shown in Figure 5a and b, with values of linear regression coefficients that show the validity of the Freundlich isotherm model on the data in Table 3. The small value of K_f is a measure of the degree or strength of adsorption, and it indicates increased adsorption [40, 41].

Based on this model, the cellulosic-based polymer PMBP in Table 3 has a better degree of adsorption than the raw PMBP. This is the basis that the modified/treated has smaller K_f values than the unmodified. This observation corroborates the findings of Ekpete et al. [41], that researched the adsorption of lead (II), copper(II) and iron(II) in a multi-metal aqueous solution by waste rubber tyres for the design of a single-batch adsorber.

The Freundlich adsorption intensity parameter, 1/n, indicates the deviation of the adsorption isotherm from linearity. If n= ¼ 1, the adsorption is linear, i.e., the adsorption sites are homogeneous and there is no interaction between the adsorbed species. If 1/n < 1, the adsorption is favourable; the adsorption capacity increases and new adsorption sites appear. If 1/n > 1, the adsorption is unfavourable; the adsorption bonds become weak, and the adsorption capacity decreases [42, 43, 44]. Table 3 shows that the 1/n values for the Cu(II)

ion in all adsorbents range from 0.8435 to 0.9125, indicating high adsorption intensity and linearity. However, the adsorption intensity due to raw PMBP for the metals considered has weak adsorption bonds and decreased adsorption capacity, based on their high 1/n values. This implies that the modified and treated PMBP are better adsorbents than the raw PMBP. These findings are consistent with those Özacar & Şengil [39) and Ekpete et al. [41], who investigated various novel adsorbents used in heavy metal removal.

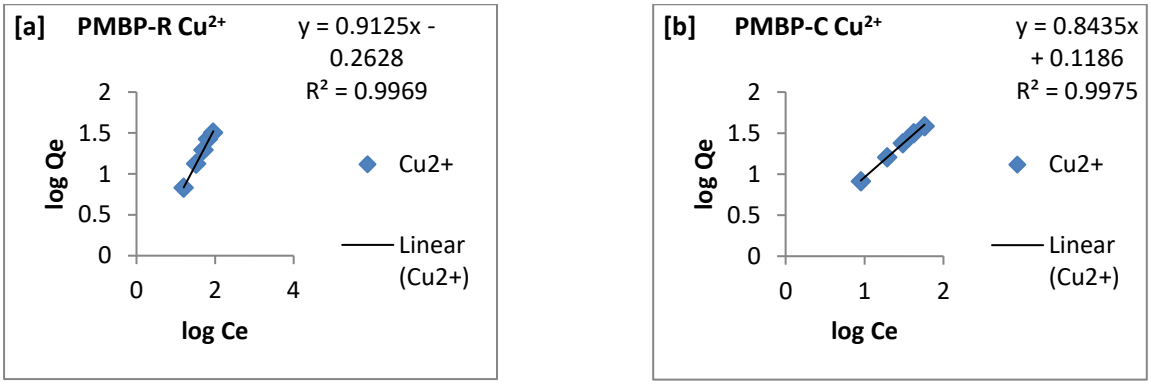

Figure 5: Freundlich adsorption of Cu^{2+} using PMBP

3.5.3 Temkin Adsorption Isotherms of Cu^{2+} Celluloic-Based Polymer of PMBP

This isotherm contains a factor that explicitly takes into account adsorbent–adsorbate interactions and is based on the assumption that the heat of adsorption (function of temperature) of all molecules in the layer would decrease linearly rather than logarithmically with coverage [45]. Table 4 extrapolates the Temkin isotherm constant of Cu(II) ions in different adsorbents from Figures 5a and b.

Table 4: Temkin Isotherm parameters for the adsorption of Cu(II) Ion on PMBP

	Adsorbents	K or b (J/mol)	A	B(J/mol)	R^2
1	PMBP-R	169.92	11.396	14.5808	0.9556
2	PMBP-C	152.157	6.1589	16.2829	0.9676

The values of b, A_T, B, and R^2 in Table 4 were extrapolated from Figure 5a and b.
B and b (J/mol) are Temkin constants related to adsorption heat, while A_T (l/mg) is the equilibrium binding constant corresponding to the maximum binding energy. The B and b were determined from the slope, whereas the A_T was obtained from the intercept [46].
The heat of adsorption (B) less than 40 kJ/mol indicates a physical adsorption, and its value of more than 40 kJ/mol represents a chemical adsorption [14, 44, 46].The relationship between the adsorbents (modified and unmodified) and the metal ions (Cu(II) ion) was within the range of physical adsorption because the heat of adsorption was less than 40 kJ/mol. These findings corroborate the work of Saini et al. [47], who investigated Cd(II) ion adsorption using unmodified and NTA-modified Dendrocalamus strictus charcoal powder. Other works found to be consistent with the result were Ekpete et al. [41], Shikuku and Mishra [46], and Patrulea et al. [48].The R^2 values for all the adsorbents and metal ions were

close to unity, which implies that the model was consistent for both modified and unmodified adsorbents [38].
An overall consideration of the R^2 values of the three isotherm models used in this research, reveals that the experimental data were consistent with all the models, but fit more to the Feundlich and Temkin models than the Langmuir isotherm. All the R2 values in both the Feundlich and Temkin models lie within the range of 0.9109–0.9992, whereas the Langmuir model has an R^2 value in the range of 0.8549–0.974.

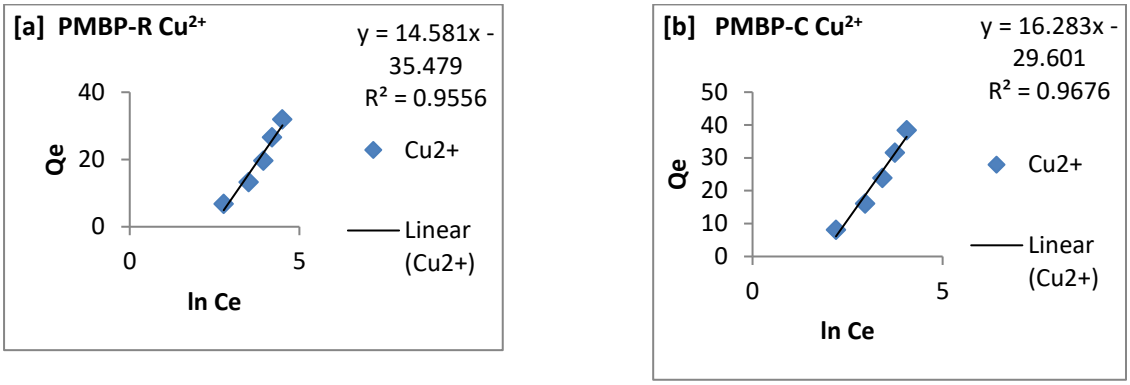

Figure 5: Temkin adsorption of Cu^{2+} using PMBP

3.6 Thermodynamic adsorption of Cu(II) ion via Celluloic-Based Polymer of PMBP

Thermodynamic parameters such as standard Gibb's free energy change (ΔG^o) for PMBP metal removal at different temperatures, enthalpy change (ΔH^o), and standard entropy change (ΔS^o) were investigated for PMBP metal removal. Table 5 shows the thermodynamic parameters for Cu(II) ion removal using raw and cellulose-based polymer of PMBP.

Table 5: Thermodynamic parameters for the adsorption of Cu(II) on PMBP

	Adsorbents	ΔH°(-KJmol^{-1})	ΔS°(-Jmol^{-1}K^{-1})	R^2	ΔG°(KJ mol^{-1})				
					303K	**308K**	**313K**	**318K**	**323K**
1	PMBP-R	12.513	42.73	0.929	-0.434	-0.654	-0.762	-1.075	-1.289
2	PMBP-C	40.323	137.75	0.9317	1.415	-2.104	-2.792	-3.485	-4.170

The values of thermodynamic parameters obtained by plotting ln KL versus 1/T (Figure 6a and b) are listed in Table 5. The negative values of Gibbs free energy for Cu (II) ion shows that the adsorption process is spontaneous and that the degree of spontaneity of the reaction increases with increasing temperature [49]. The modified/treated adsorbents have higher ΔG° values than the unmodified PMBP adsorbent. This implies that the modified/treated contains more adsorbate, which is shown as increased ΔG° values. Table 5 also shows that an increase in temperature leads to an increase in the value of ΔG°. These findings were consistent with Azouaou et al. [38] thar researched on Cd(II) removal via unmodified and NTA-modified *Dendrocalamus* strictus charcoal powder and Cherono et al.'s [49] study of waste rubber tyre as an adsorbent of Pb(II), Cu(II), and Fe(II) ions.

It has been reported that, ΔG° values up to -20 kJ/mol are consistent with the electrostatic interaction between sorption sites and the metal ion (physical adsorption), while ΔG° values more negative than -40 kJ/mol involve charge sharing or transfer from the surface of the metal ion to form a coordinate bond (chemical adsorption)[40]. The ΔG° values obtained in this study for modified and unmodified for all the metals investigated at the range of temperatures of 303K–323K were all less than -5 kJ/mol, which indicates that physical adsorption was the predominant mechanism in the sorption process [39, 42].

The adsorption enthalpies of both cellulose-based polymers and raw PMBP in Table 5 have negative values, and both seem to be exothermic in nature. The ΔH^o values of the cellulose-based polymer PMBP for Cu(II) ion were higher than the raw PMBP. This implies that cellulose-based polymer contained more adsorbate than the raw material at a given concentration of the adsorbent. This observed increase in ΔH^o is consistent with Mustapha et al. [50], who worked on *Albizia lebbeck* pods used in the adsorption of Pb(II), Cu(II), Cd(II) and Zinc(II). The ΔH^o values analysis for this study as shown in Table 4.13 reveals that PMBP-RM and PMBP-C were better adsorbent for Cu(II) ion, since they have the ΔH^o values of 40.323KJ/mol and 31.582KJ/mol. PMBP-C and PMBP-RM were the most preferred adsorbents for Pb(II), based on the ΔH^o values of 38.054 KJ/mol and 37.865 KJ/mol, while PMBP-AC and PMBP-C were better adsorbents for Fe(II), with the ΔH^o values of 30.922 KJ/mol and 24.928 KJ/mol.

The adsorption entropy of both modified/treated and unmodified PMBP in Table 5 has negative values and indicates less disorder and randomness due to an association between the adsorbent and the adsorbate during adsorption. This negative ΔS^o for both modified and unmodified lignin is in line with Okoronkwo and Oluseun [51], who worked on the biosorption of different metals using unmodified and modified lignin extracted from agricultural waste. From Table 5, the ΔS^o values for cellulose-based polymer adsorbents are higher than the unmodified PMBP. This implies that the loss of randomness is a result of an increase in the adsorbent-adsorbate interface during the adsorption process [52].

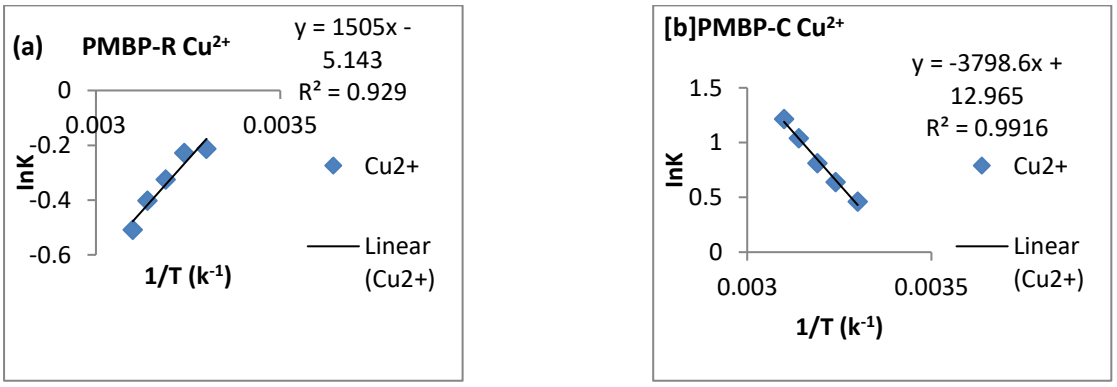

Figure 6: Thermodynamic adsorption of Cu^{2+} using PMBP

3.7 Adsorption Kinetic Studies of PMBP

Adsorption kinetics describes the relationship between adsorbent and adsorbate as well as the rate of adsorption with respect to time. In order to define the adsorption kinetics of heavy

metal ions, the kinetic parameters for the adsorption processes were studied for the contact times ranging between 1 to 150 minutes, and first-order, second-order, and intra-particle diffusion models were applied to experimental dataTable 4.14 contains the maximum adsorbate in the adsorbent calculated ($q_{cal.}$), the experimented adsorbate in the adsorbent (qexp.), the rate constant of the pseudo first order adsorption process (K_1), the rate constant of the pseudo second order adsorption process (K_2), the intraparticle diffusion rate constant (K_d), and R^2 for different models, which are extrapolated from Figure 7.

Table 4.14 Kinetic parameters for the adsorption of Cu(II) ion on PMBP

Adsorbents	First Order			Second Order			Intra Particle Diffusion		
	k1(min-1)	qcalc (mg/g)	R^2	k2(g/mg1min-1)	qcalc (mg/g)	R^2	kd(mgl−1 min−1/2)	R^2	$q_{exp.}$ (mg/g)
PMBP-R	-0.0016	3.294	0.985	0.0304	7.622	0.9992	0.0795	0.9621	7.1848
PMBP-C	-0.0035	1.352	0.9848	0.0442	9.3197	0.9990	0.063	0.9892	9.0026

The rate constant for the pseudo first order adsorption process (K_1) was obtained by plotting ln (qe-qt) versus time. The value of K_1 was extrapolated from the slope, whereas the maximum adsorbate of the adsorbent was obtained as the intercept. Figure 7 depicts negative graphs for the pseudo-first-order adsorption process for Cu(II).This implies that an increase in time leads to a decrease in the change adsorption capacity at equilibrium. The comparison of the experimentally determined adsorption capacity ($q_{exp.}$) and the calculated maximum adsorbate ($q_{cal.}$) of the pseudo first-order adsorption shows that the adsorption did not follow the pseudo first order. This is based on the wide range of differences found in the experimental and calculated values of each of the adsorbates in the raw and cellulose-based polymer PMBP adsorbent. In-line with this finding was the research of Rahangdale and Kumar (2018) who researched on the removal of cadmium using modified and unmodified carbohydrate polymers from Chitosan, and also Mustapha et al. [50] who worked on a comparative study for the removal of cadmium(II) ions using unmodified and NTA-modified Dendrocalamus strictus charcoal powder.

The pseudo-second-order adsorption rate constant (K_2) was studied with a plot of t/q vs. t (Figure 8a and b). The slope was used to calculate the maximum adsorbate of the adsorbent, and the intercept was used to calculate K_2. The experimented adsorption capacity ($q_{exp.}$) and the calculated maximum adsorbate ($q_{cal.}$) of pseudo second order gave equivalent values for each of the metals and the adsorbents (modified and unmodified). This implies that the adsorption of Cu(II) ion with PMBP adsorbents followed a pseudo-second order adsorption process. This is consistent with the research of Qing [53] and Shilpi [54], who researched metal removal using natural biomass, with an adsorption kinetics that was achieved through pseudo-second order adsorption.

The intra-particle diffusion was observed using the relationship between specific sorption (q) and the square root of time ($t^{1/2}$) (Figure 9a and b). Where K_d is the rate of sorption controlled by intra particle diffusivity (mgg^{-1} min-1(1/2)), and C depicts the boundary layer thickness [38]. This model predicts that the plot of qt versus $t^{1/2}$ should be linear with k_d and C as slope and intercept, respectively, if intra-particle diffusivity is involved in the sorption process [55, 56].

According to Adams et al. [56] and Azouaou et al. [38], the intra-particle diffusivity plot for sorption mechanism assumes an intra-particle diffusivity model if the following conditions

are met: (i) High R^2 values to ascertain applicability. (ii) Straight line that passes through the origin for the plot area qt versus $t^{1/2}$ (iii) Intercept C< 0.

Figure 7 depicts Cu(II) ion intraparticle diffusion. From the figures, the straight line did not pass through the origin, and the constant C, that is, the intercept in the graphs, is greater than zero (C>0). As a result, the model cannot explain the adsorption of Cu(II) ions using PMBP adsorbents. However, the presence of high correlation coefficient values (R^2) indicates the multiple adsorption stages and the suggestion that pore diffusion was involved [56].

This is in line with the findings of Elijah et al. [44] and Saini et al. [47], who investigated the intra-particle diffusivity model adsorption mechanism of Ni(II), Cd(II), Co(II), and Cu(II) ions with carbonised star apple and natural biomass. Their founding suggests that the model does not favour adsorption as a result of the non-compliance of the (1) straight line, which passes through the origin for the plot area qt versus $t^{1/2}$. (i) Intercept C< 0

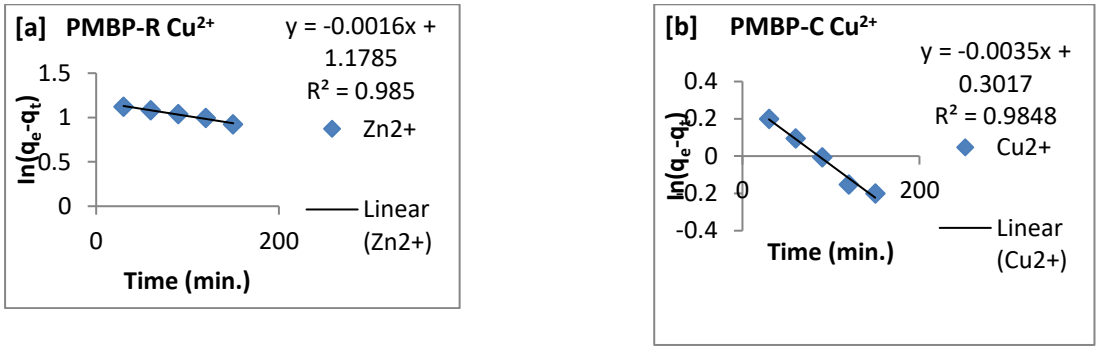

Figure 7: Pseudo-first-order plots for Cu(II) ion removal at different times

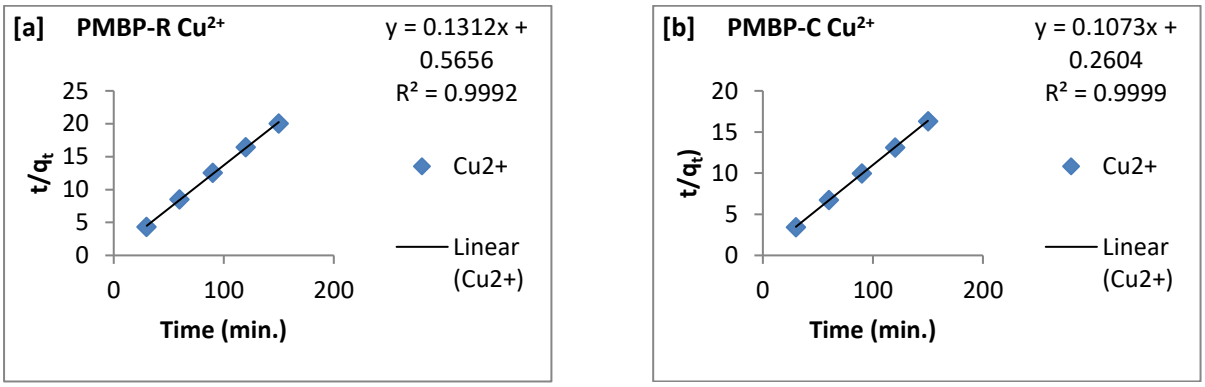

Figure 8: Pseudo-second-order plots for Cu(II) ion removal at different times

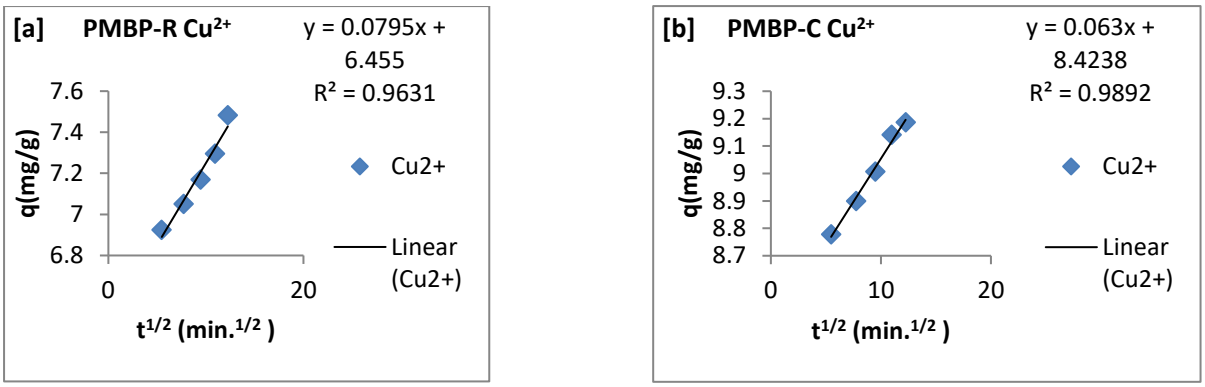

Figure 9: Plots for evaluating intra particle diffusion rate constant of Cu (II) ion

4 Conclusion

Cellulose was successfully isolated from PMBP biomass waste *via* delignification and bleaching. XRD, SEM, TGA, DGA, and FTIR measurements of the isolated cellulose revealed some level of removal of hemicellulose and lignin from the raw PMBP powder. The crystallinity, morphological properties, stability, and function group of both raw and isolated cellulose were compared. The thermogravimetric analysis demonstrated that the isolated cellulose has enhanced thermal stability over the raw PMBP powder. The results of this study suggest that PMBP biomass can constitute an alternative raw material for cellulose polymer reinforcement composites.

The adsorption isotherms, kinetic and thermodynamic studies show that the cellulosic-based polymer has better copper (II) ion removal capacity than the raw PMBP. The study was based on the availability, cheapness, and non-toxic nature of PMBP, and the results of the study recommend the use of a cellulosic-based polymer obtained from PMBP for Cu(II) ion removal.

Ethics approval and consent to participate

Note applicable

Consent for publication

Not applicable

Availability of data and material

The datasets that were used and/or analyzed for this study are included in this manuscript, and others not included in the manuscript can be requested from the corresponding author.

Acknowledgements

I wish to thank the department of chemistry at the Enugu State University of Science and Technology, and the Ignatius Ajuru University of Education, Rivers State, Nigeria, for making the laboratory and the departmental library available within the period of this work.

Competing Interests

The authors declare that they have "no competing interests" in this article.

Funding

All the funds used in each stage, that is, isolation, characterization, and adsorption studies, were personal funds from the three authors.

Authors' Contributions

NPO and OKJ conducted the experiment on the isolation of cellulose-based polymers from PMBP. The interpretation of the spectra of both raw and isolated cellulose was done by OKJ and OE. The adsorption study was conducted by NPO and OE. The extrapolation of the data from the model was jointly achieved by the three authors. OKJ wrote the manuscript, but it was proofread and approved for submission by NPO and OE.

Authors' information

Dr. Nsude P. O. is a polymer/physical chemist and a senior lecturer in the Department of Industrial Chemistry, Enugu State University of Science and Technology,Enugu State, Nigeria. Dr. Orie K. J. is an organic chemist and holds the rank of lecturer 1 in the Department of Chemistry at the Ignatius Ajuru University of Education, Rivers State, Nigeria. Dr. Owhoeke E. is an environmental chemist and a lecturer 1, in the Department of Industrial Chemistry/Petrochemical Technology, University of Port Harcourt, Nigeria.

References

1. Saravanan A, Karishma S, Kumar P S, Varjani S, Yaashikaa PR, Jeevanantham S, Reshma B (2021) Simultaneous removal of Cu (II) and reactive green 6 dye from wastewater using immobilized mixed fungal biomass and its recovery. *Chemosphere*, 271:129519. https://doi.org/10.1016/j.chemosphere.2020.129519
2. Shaikh HM, Anis A, Poulose AM, Al-Zahrani SM, Madhar NA, Alhamidi A, Alam MA (2021) Isolation and characterization of alpha and nanocrystalline cellulose from date palm (Phoenix dactylifera L.) trunk mesh. Polymers, 13(11):1893-99. https://doi.org/10.3390/polym13111893
3. Zhu HX, Cao XJ, He YC, Kong QP, He H, Wang J (2015) Removal of Cu^{2+} from aqueous solutions by the novel modified bagasse pulp cellulose: Kinetics, isotherm and mechanism. Carbohydrate polymers, 129:115-126 https://doi.org/10.1016/j.carbpol.2015.04.049
4. Nsude OP, Agboeze E, Ezeh EC, Ike OC, Omuluche OC, Orie KJ, Ogbobe O (2022) Isolation and characterization of cellulose from Pentaclethra macrophylla Benth pod biomass wastes for polymer reinforcement composite. J Chem Soc Nig 47(3). https://doi.org/10.46602/jcsn.v47i3.765
5. Khandelwal M, Windle AH (2013) Hierarchical organisation in the most abundant biopolymer–cellulose. MRS Online Procs Lib (OPL), 1504, mrsf12-1504. https://doi.org/10.1557/opl.2013.379
6. Akinlabu DK, Owoeye TF, Owolabi FE, Audu OY, Ajanaku CO, Falope F, Ajani OO (2019). Phytochemical and Proximate Analysis of African Oil Bean (Pentaclethra macrophylla Benth) Seed. J Physics: Conf Series 1378(3): 032057-66. 10.1088/1742-6596/1378/3/032057
7. Fernández, PM, Viñarta SC, Bernal AR, Cruz EL, Figueroa LI (2018) Bioremediation strategies for chromium removal: current research, scale-up approach and future perspectives. Chemosphere, 208:139-148. https://doi.org/10.1016/j.chemosphere.2018.05.166

8. Madukasi EI, Tojola OB, Oso K, Igwe CC (2015) Thermo-chemical features of coating sludge and codensification of ad alternative energy source. AASCIT J Env, 1(2): 28-34.
9. Alothman OY, Kian LK, Saba N, Jawaid M, Khiari R (2021) Cellulose nanocrystal extracted from date palm fibre: Morphological, structural and thermal properties. Ind Crops Products, 159: 113075. https://doi.org/10.1016/j.indcrop.2020.113075
10. Ayanda OI, Dedeke GA, Ekhator UI, Etiebet MK (2018) Proximate composition, structural characterization and phytochemical screening of the seed oil of adenanthera pavonina linn. Rasayan J Chem, 1-7.
11. Velmurugan R, Muthukumar K (2012) Ultrasound-assisted alkaline pretreatment of sugarcane bagasse for fermentable sugar production: optimization through response surface methodology. Bioresource Techn *112*: 293-299. https://doi.org/10.1016/j.biortech.2012.01.168
12. Basha CA, Bhadrinarayana NS, Anantharaman N, Begum KMS (2008) Heavy metal removal from copper smelting effluent using electrochemical cylindrical flow reactor. J Hazardous Mat 152(1): 71-78. https://doi.org/10.1016/j.jhazmat.2007.06.069
13. Choudhary B, Paul D (2018) Isotherms, kinetics and thermodynamics of hexavalent chromium removal using biochar. J Env Chem Engr, 6(2): 2335-2343. https://doi.org/10.1016/j.jece.2018.03.028
14. Nsude OP, Orie KJ (2022) Microcrystalline Cellulose of Oil Bean Pod: Extraction, Physico-chemical, Brunauer–Emmett–Teller (BET), and Flow-ability Analysis. Asian J Applied Chem Res, 12(4): 1-12. https://doi.org/10.9734/ajacr/2022/v12i4226
15. Vardhan H, Verma G, Ramani S, Nafady A, Al-Enizi AM, Pan Y, Ma S (2018) Covalent organic framework decorated with vanadium as a new platform for Prins reaction and sulfide oxidation. ACS Applied Mat & Interfaces, 11(3): 3070-3079. https://doi.org/10.1021/acsami.8b19352
16. Sathiyavimal S, Vasantharaj S, Bharathi D, Saravanan M, Manikandan E, Kumar SS, Pugazhendhi A (2018) Biogenesis of copper oxide nanoparticles (CuONPs) using Sida acuta and their incorporation over cotton fabrics to prevent the pathogenicity of Gram negative and Gram positive bacteria. J Photochem Photobio B: Bio, 188: 126-134. https://doi.org/10.1016/j.jphotobiol.2018.09.014
17. Kumar A, Negi, YS, Choudhary V, Bhardwaj NK (2014) Characterization of cellulose nanocrystals produced by acid-hydrolysis from sugarcane bagasse as agro-waste. J Mat Phy Chem 2(1): 1-8. doi: 10.12691/jmpc-2-1-1.
18. Ramrakhiani L, Majumder R, Khowala S (2011) Removal of hexavalent chromium by heat inactivated fungal biomass of Termitomyces clypeatus: Surface characterization and mechanism of biosorption. Chem Engr J, 171(3):1060-1068. https://doi.org/10.1016/j.cej.2011.05.002
19. Anitha A, Sowmya S, Kumar PS, Deepthi S, Chennazhi KP, Ehrlich H, Jayakumar R (2014). Chitin and chitosan in selected biomedical applications. Progress in Polymer Sci 39(9) 1644-1667. https://doi.org/10.1016/j.progpolymsci.2014.02.008
20. Saravanan R, Khan MM, Gupta VK, Mosquera E, Gracia F, Narayanan V, Stephen C (2015) ZnO/Ag/CdO nanocomposite for visible light-induced photocatalytic

degradation of industrial textile effluents. J Colloid Interface Sci 452: 126-133. https://doi.org/10.1016/j.jcis.2015.04.035
21. Suganya S, Kumar PS (2018) Kinetic and thermodynamic analysis for the redemption of effluents containing Solochrome Black T onto powdered activated carbon: a validation of new solid-liquid phase equilibrium model. J Mol Liquids, 259: 88-101. https://doi.org/10.1016/j.molliq.2018.03.004
22. Abulude FO, Ogunmola DN, Alabi MM, Abdulrasheed Y (2018) Atmospheric deposition: Effects on sculptures. Chem Int 4(2): 136-145.
23. Ohwoavworhua FO, Adelakun TA, Okhamafe AO (2009) Processing pharmaceutical grade microcrystalline cellulose from groundnut husk: Extraction methods and characterization. Int J Green Pharm (IJGP), 3(2).
24. Nwabanne JT, Igbokwe PK (2012) Comparative study of lead (II) removal from aqueous solution using different adsorbents. Int J Engr Res Appl 2(4): 1830-1838.
25. SinghSR, Singh AP (2012) Treatment of water containing chronium (VI) using Rice husk carbon as a new low cost Adsorbent. Int J Env Res 6(4):917-924.
26. Rao MM, Ramana D, Seshaiah K, Wang M, Chang S, Chien (2009) Removals of some metal ions by activated carbon prepared from Phaseolus aureus hulls. J Hazard matter 166: 1006-1013. https://doi.org/10.1016/j.jhazmat.2005.08.018
27. Akinjokun AI, Petrik LF, Ogunfowokan AO, Ajao J, Ojumu TV (2021) Isolation and characterization of nanocrystalline cellulose from cocoa pod husk (CPH) biomass wastes. Heliyon, 7(4): e06680. https://doi.org/10.1016/j.heliyon.2021.e06680
28. Rosli NA, Ahmad I, Abdullah I (2013) Isolation and characterization of cellulose nanocrystals from Agave angustifolia fibre. BioResources 8(2): 1893-1908
29. Mbata T, Orji MU, (2008) Process optimization in the production and preservation of ugba, a Nigerian fermented food. Int. J. Microbiol, 4: 2-6.
30. Sheltami RM, Abdullah I, Ahmad I, Dufresne A, Kargarzadeh H (2012) Extraction of cellulose nanocrystals from mengkuang leaves (Pandanus tectorius). Carbohydrate Polymers 88(2):772-779. https://doi.org/10.1016/j.carbpol.2012.01.062
31. Nsude OP, Orie KJ, Udeozo PI, Ogbobe O, Chime CC (2022) Isolation, physicochemical and BET analysis of cellulose from Pentaclethra macrophylla Benth (Oil Bean) pod biomass wastes. Int Res J Pure and Applied Chem 12(5): 9-22. DOI: 10.9734/IRJPAC/2022/v23i530474
32. Costa-Silva TA, Souza CRF, Said S, Oliveira WP (2015) Drying of enzyme immobilized on eco-friendly supports. Afri J Biotechn 14(44): 3019-3026. DOI: 10.5897/AJB2015.14830
33. AIkinjokun A, Petrik LF, Ogunfowokan AO, Ajao J, Ojumu TV (2021) Isolation and characterization of nanocrystalline cellulose from cocoa pod husk (CPH) biomass wastes. Heliyon, 7(4): e06680. https://doi.org/10.1016/j.heliyon.2021.e06680

34. Donlawson C, Nweneka DO, Orie KJ, Okah R (2020) Synthesis and Bioactivity of 1-((2-Carbamoylguanidino)(furan-2-ylmethyl) urea. Am J Anal Chem 11(7): 280-288. DOI: 10.4236/ajac.2020.117022

35. Rivai AA, Siregar VP, Agus SB, Yasuma H (2018) Analysis of habitat characteristics of small pelagic fish based on generalized additive models in Kepulauan Seribu Waters. In IOP Conf Series: Earth and Env Sci (Vol. 139, No. 1, p. 012014). IOP Publishing. DOI 10.1088/1755-1315/139/1/012014

36. Ushakumary ER, Madhu G (2013) Waste water treatment using low cost natural adsorbents. *Doctoral dissertation, Cochin University Of Science And Technology).*
37. Volesky B (2003) Sorption and biosorption. *St. Lambert, Québec: BV Sorbex.*

38. Azouaou N, Sadaoui Z, Djaafri A, Mokaddem M (2010) Adsorption of cadmium from aqueous solution onto untreated coffee grounds: Equilibrium, kinetics and thermodynamics. J Hazardous mat , 184*(1-3):*126-134. https://doi.org/10.1016/j.jhazmat.2010.08.014

39. Özacar M, Şengil IA (2003) Adsorption of reactive dyes on calcined alunite from aqueous solutions. J Hazardous mat, , *98(1-3)* (211-224). https://doi.org/10.1016/S0304-3894(02)00358-8

40. Horsfall JM, Abia AA, Spiff AI (2006) Kinetic studies on the adsorption of Cd2+, Cu2+ and Zn2+ ions from aqueous solutions by cassava (Manihot sculenta Cranz) tuber bark waste. Bioresource techn *97(2) :*283-291 https://doi.org/10.1016/j.biortech.2005.02.016

41. Ekpete OA, Horsfall JM, Spiff AI (2011) Fixed bed adsorption of chlorophenol on to fluted pumpkin and commercial activated carbon. Austr J Basic Applied Sci, 5(11) *:*1149-1155.

42. Adediran GO, Tella AC, Mohammed HA (2007) Adsorption of Pb, Cd, Zn, Cu and Hg ions on formaldehyde and pyridine modified bean husks. J Applied Sci Env Management, , *11(2).* DOI: 10.4314/jasem.v11i2.55019

43. Isa MH, Lang LS, Asaari FA, Aziz HA, Ramli NA, Dhas JP (2007) Low cost removal of disperse dyes from aqueous solution using palm ash. Dyes and pigments , 74(2): 446-453. https://doi.org/10.1016/j.dyepig.2006.02.025

44. Elijah LK, Junior HM, Ibuteme SA (2015) Speciation of some heavy metals in sediments of the Pennington River, Bayelsa State, Nigeria. Am. Chem Sci J 5: 238-246. DOI: 10.9734/ACSj/2015/14696

45. Ragadhita R, Nandiyanto AB (2021) How to calculate adsorption isotherms of particles using two-parameter monolayer adsorption models and equations. *Indonesian J Sci Techn, 6(1):*205-234. : https://doi.org/10.17509/ijost.v6i1.32354

46. Shikuku VO, Mishra T (2021) Adsorption isotherm modeling for methylene blue removal onto magnetic kaolinite clay: a comparison of two-parameter isotherms. Applied Water Sci 11(6): 1-9 https://doi.org/10.1007/s13201-021-01440-2

47. Saini S, Katnoria JK, Kaur I (2019) A comparative study for removal of cadmium (11) ions using unmodified and NTA-modified Dendrocalamus strictus charcoal powder. J Env Health Sci Engr. 17(1):259-272. https://doi.org/10.1007/s40201-019-00345-2

48. Patrulea V, Negrulescu A, Mincea MM, Pitulice LD, Spiridon OB, Ostafe V (2013) Optimization of the removal of copper (II) ions from aqueous solution on chitosan and cross-linked chitosan beads. BioResources 8(1)*:* 1147-1165

49. Cherono F, Mburu N, Kakoi B (2021) Adsorption of lead, copper and zinc in a multi-metal aqueous solution by waste rubber tires for the design of single batch adsorber. Heliyon 7(11*)* (e08254). https://doi.org/10.1016/j.heliyon.2021.e08254

50. Mustapha S, Shuaib DT, Ndamitso MM., Etsuyankpa MB, Sumaila A, Mohammed UM, Nasirudeen MB (2019) Adsorption isotherm, kinetic and thermodynamic studies for the removal of Pb (II), Cd (II), Zn (II) and Cu (II) ions from aqueous solutions using Albizia lebbeck pods. *Applied Water Sci 9*, 1-11. https://doi.org/10.1007/s13201-019-1021-x

51. Okoronkwo A E, Olusegun SJ (2013) Biosorption of nickel using unmodified and modified lignin extracted from agricultural waste. Desalination and Water Treatment , 51(7-9): 1989-1997. https://doi.org/10.1080/19443994.2012.714896
52. Zhou Y, Zhang L, Fu S, Zhan H (2012) Adsorption behaviour of Cd(ii), Pb(ii) and Ni(ii) from aqueus solution on cellulose based hydrogels. *Bioresourses 7* (3).

53. Qing C (2010) Study on the adsorption of lanthanum(iii) from aqueous solution by bamboo charcoal. J Rare Earths 28:125-131. https://doi.org/10.1016/S1002-0721(10)60272-4

54. Shilpi K (2013) Sorption mechanism of Cd(ii) and Zn(ii) onto modified palm shell. Adsorption Sci and Techn 31(6):503-520

55. Orie, K. J., & Christian, M. (2015). The corrosion inhibition of aluminium metal in 0.5 M sulphuric acid using extract of breadfruit peels. *International Research Journal of Engineering and Technology (IRJET)*, *2*(8), 2395-0072.

56. Adams IU, Abdulrahman FW, Hassan LG, Itodo HU (2010) Physiochemical parameters of adsorbents from locally sorted H3PO4 and ZnCl2 modified agricultural wastes. *New York Sci J , 3* (5).